nature cell biology

DOI: 10.1038/ncb2163

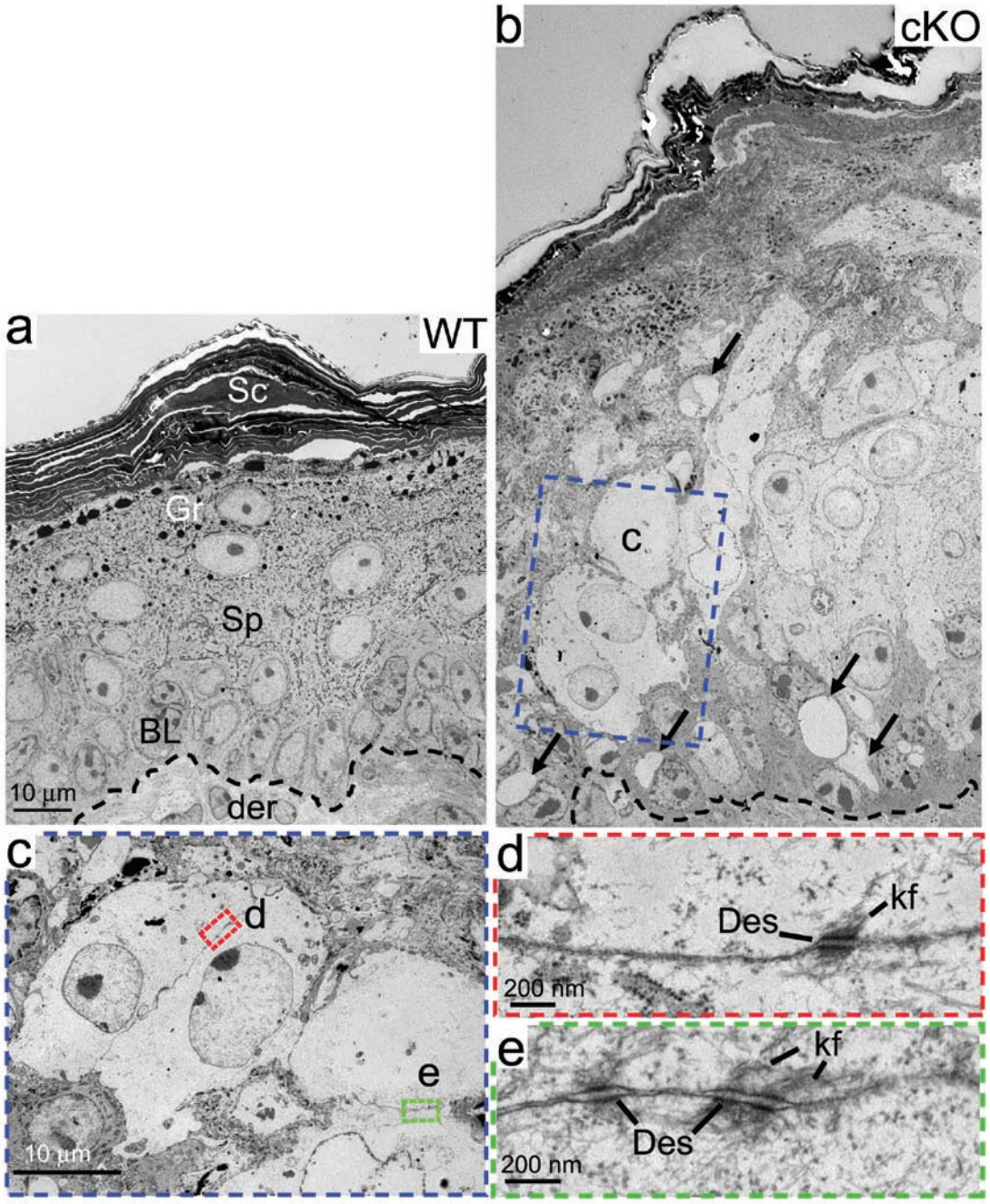

Figure S1 Srf-deficient newborn epidermis is grossly defective and yet cells within the tissue still display typical signs of adhesion. Ultrastructural analysis of WT (a) and Srf-cKO (b) epidermis. Arrows indicate vacuoles, prevalent by newborn, which could be mistaken for adhesive gaps at the light microscopic level. Morphology shows grossly disorganized epidermis. (c) Boxed area in (b) is shown at higher magnification. (d-e) Boxed areas in (c) are shown at higher magnification. Kf, keratin filaments; Des, desmosome; Der, dermis; BL, basal layer; SP, spinous layer; Gr, granular layer; Sc, stratum corneum. Bars=10µm

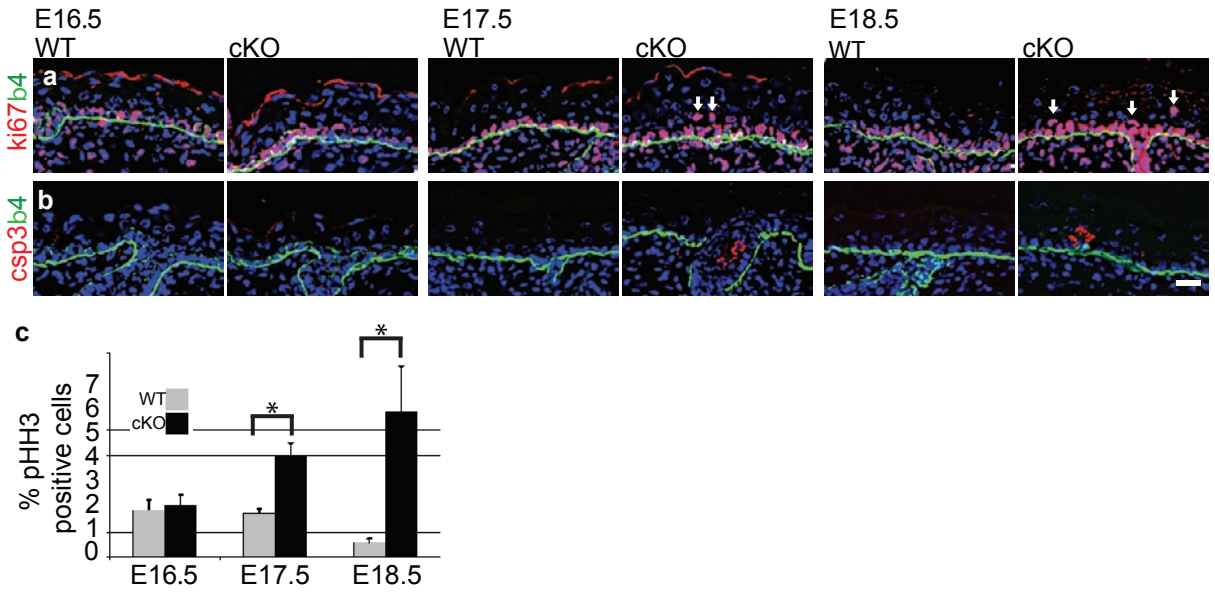

Figure S2 Elevated proliferation and apoptosis in *Srf*-cKO epidermis is evident beginning at E17.5. (a-f) Immunofluorescence of frozen backskin sections (10 μm) from E16.5-E18.5 embryos labeled with: (a) Ki67, indicative of S and M-phase cells and β4 integrin, a hemidesmosomal component (arrows denote suprabasal mitoses); and(b) active caspase3 and β4 integrin. (c) Quantifications of phospho-histone H3 (pHH3)-positive cells, reflective of early mitosis. *indicates statistically significant differences between WT and cKO. E17.5: p=0.012; E18.5: p=0.037.

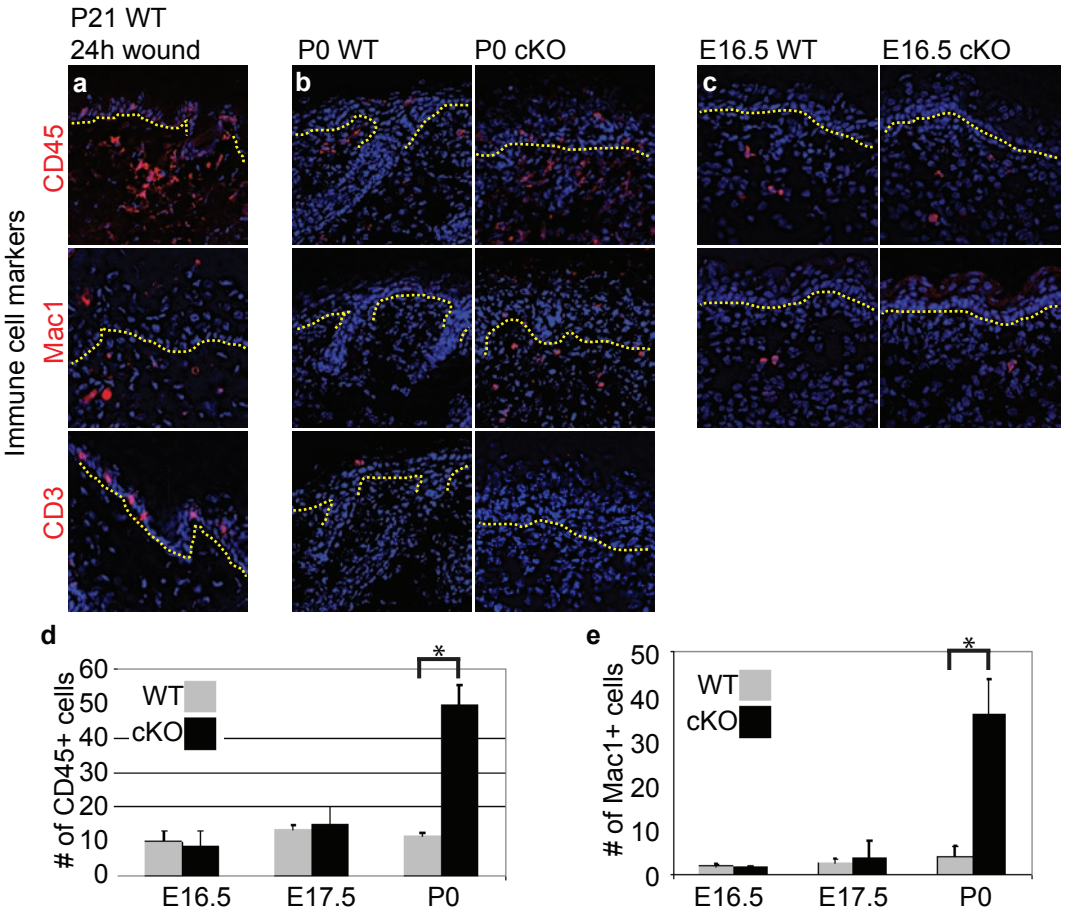

Figure S3 Signs of inflammation in the skin are not appreciable until late after *Srf* ablation during epidermal embryogenesis. (a) Wound-induced inflammatory response in P21 CD1 mouse (positive control). 24h after wounding, backskin sections were frozen, sectioned (10 µm) and processed for immunofluorescence with CD45, Mac1 and CD3 antibodies. (b-c) Unwounded E16.5 and newborn WT and *Srf-cKO* embryos were frozen, sectioned and processed for immunofluorescence as in (a). Dotted lines denote dermo-epidermal boundary. Bar=20µm. (d-e) Quantifications of the CD45 and Mac1 positive immune cells in the skin of E16.5, E17.5 and newborn mice. * indicates statistically significant differences between WT and cKO: CD45, p=0.014; Mac1, p=0.007.

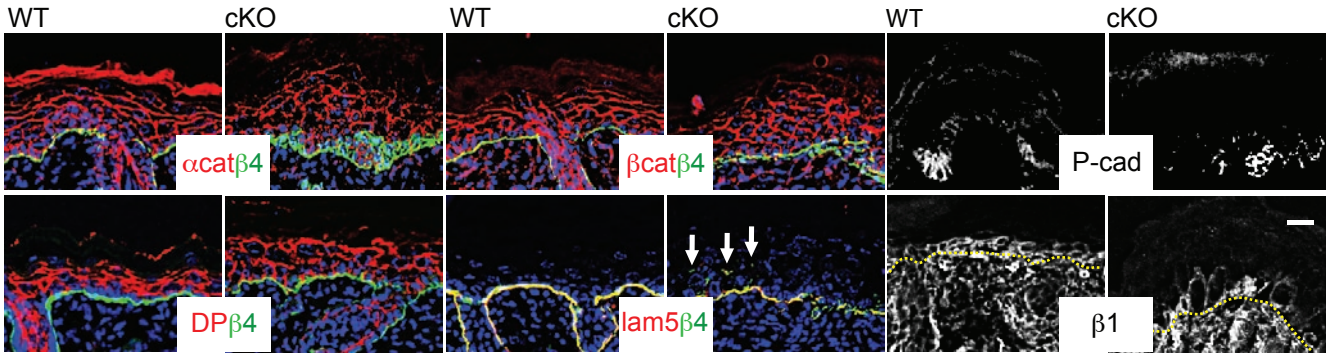

Figure S4 Normal distribution of adhesion proteins in newborn *Srf*-cKO skin. Backskin sections from newborn mice were frozen, sectioned (10 μm) and processed for immunofluorescence with α- and β-catenin, (αcat, βcat) P-cadherin (P-cad), desmoplakin (DP), Laminin 5α, and β4 and β1 integrins (β4, β1). Note overall normal distribution of these proteins. Arrows denote suprabasal laminin 5α and β4 integrin. Dotted lines denote dermo-epidermal boundaries. Bar=20μm.

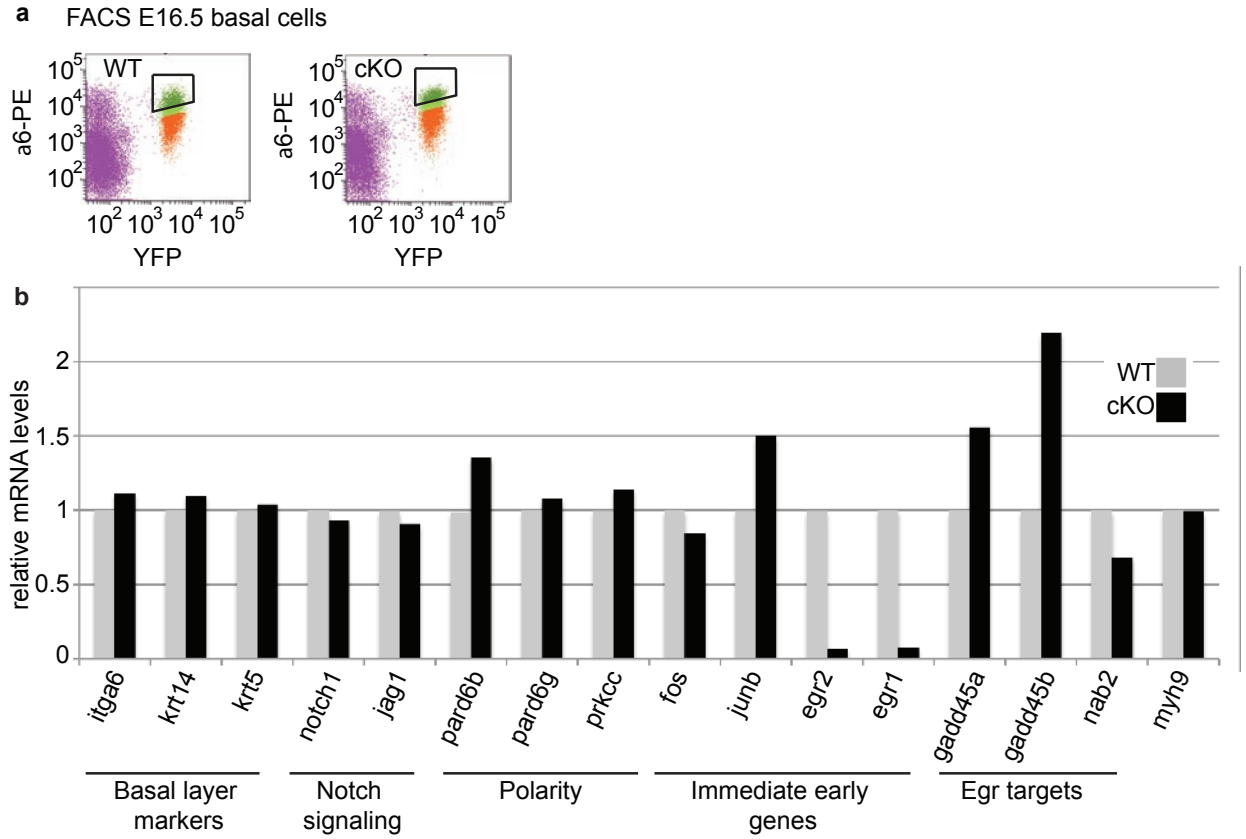

Figure S5 Most early transcriptional changes in basal cells depleted of Srf involve regulators of actomyosin and not cell cycle, inflammation, apicobasal polarity, or Notch signaling genes. (a) Fluorescence activated cell sorting (FACS) profile depicting populations of E16.5 basal cells used for microarray analyses. Embryos were from *K14-Cre* X *Rosa26YFP fl/fl* (WT) and *K14-Cre* X *Rosa26YFP fl/fl* X *Srf fl/fl* (cKO) strains. Basal cells active for Cre recombinase expressed YFP and were enriched for surface α6 integrin (green). (b) Verification of the array results by semiquantitative RT-PCR of mRNAs from FACS-purified E16.5 basal progenitors. n=2. See Table 1 and Fig. 5a for additional details.

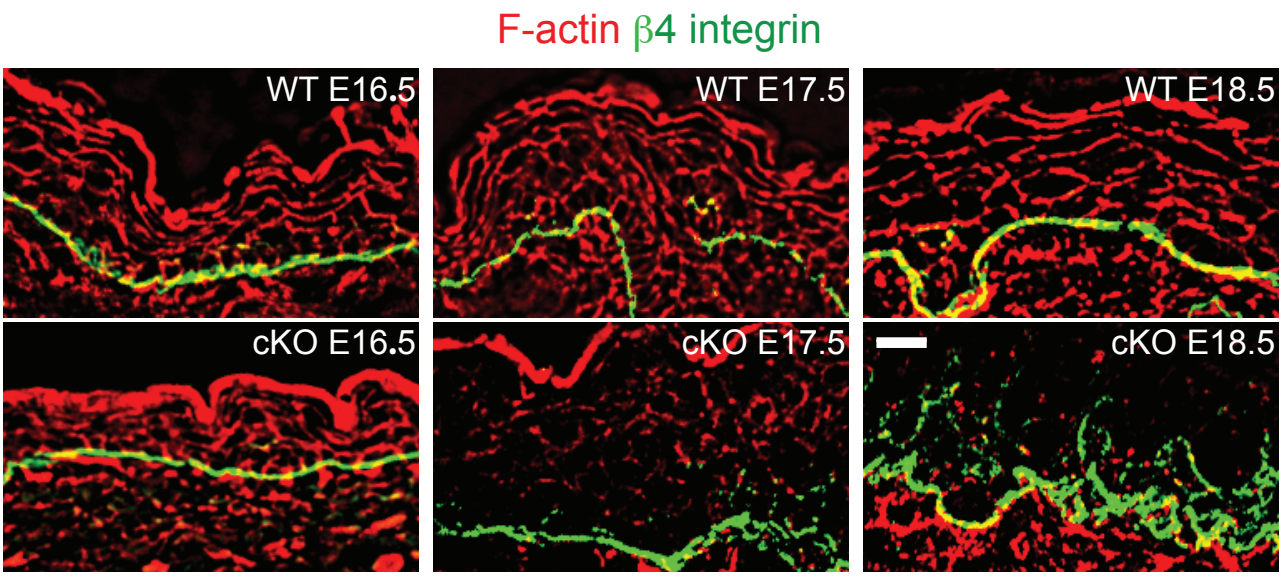

Figure S6 Alterations the actin cytoskeleton during the development of *Srf-cKO* embryos. backskin sections from E16.5, E17.5 and E18.5 mice were frozen, sectioned (10 μm) and processed for immunofluorescence**.** Phalloidin staining to mark F-actin (red) and β4 integrin (green). Note the progressive loss of F-actin staining. Bar=20μm

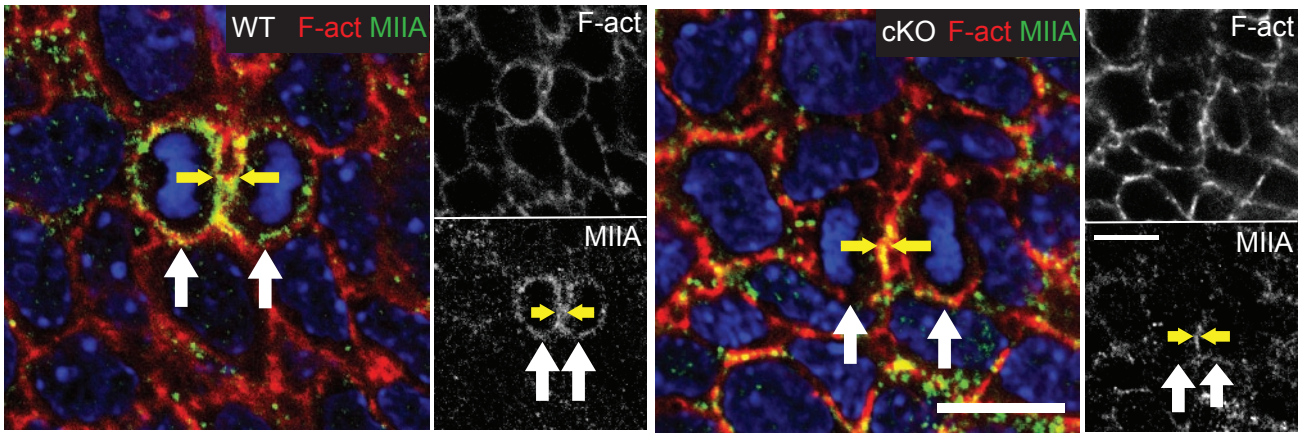

Figure S7 Normal recruitment of myosin-IIA at the midzone of late mitotic cells deficient for Srf. WT and *Srf*-cKO E16.5 embryos were subjected to whole-mount fluorescence microscopy for F-actin (phalloidin), myosin-IIA (MIIA), and DAPI. Shown are planar images through the basal layer. White arrows indicate late mitotic cells, enriched in MIIA in WT but not *Srf*-cKO. Yellow arrows indicate mid-zone enriched for MIIA in both WT and cKO samples. Bar=10μm.

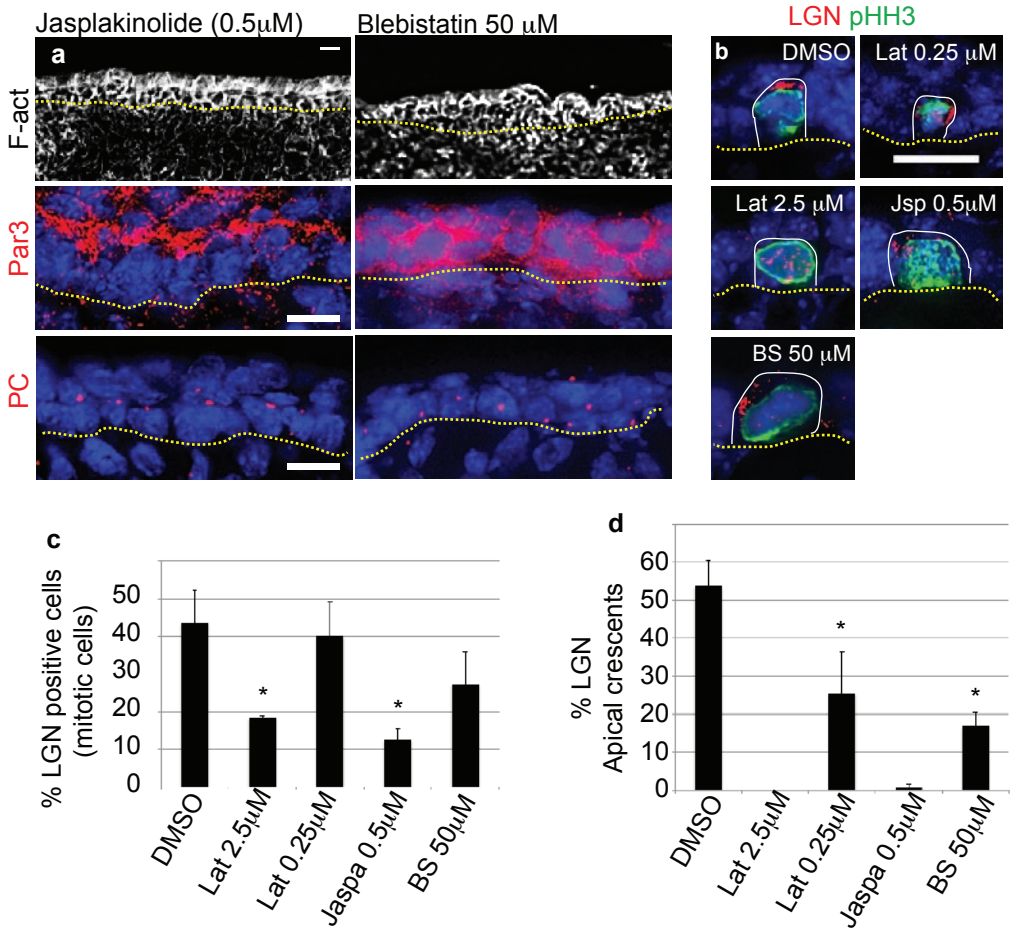

Figure S8 LGN localization is sensitive to perturbations in actin dynamics and myosin motor activity. Live E14.5 CD1 mouse embryos were placed directly into culture medium and treated with DMSO, latrunculin (Lat 2.5μM and 0.25μM), jasplakinolide (Jsp 0.5μM or blebistatin (BS, 50μm) for 1 hour at 37°C. Embryos were then frozen in OCT, sectioned (10μm) and processed for fluorescence microscopy: (a) F-actin (grayscale, phalloidin staining), Par3 and pericentrin (PC) (red). For the DMSO and latrunculin treatments, see Fig. 5 and main text. (b) Phosphohistone H3 (pHH3)(green), LGN (red) and DAPI depicting representative examples of immunolocalization. Dotted line denotes dermo-epidermal boundary. Bars=20μm. (c) Quantifications of the experimental analyses, showing percentages of early mitotic cells (pHH3+) in which LGN can be detected by immunolabeling. * indicates $p<0.05$. DMSO vs Lat 2.5μm $p=0.035$ DMSP vs Jsp 0.5μm $p=0.029$.(d) Percentages of early mitotic cells (pHH3+) in which LGN exhibited an apical crescent. * indicates $p<0.05$. DMSO vs Lat 0.25μm $p= 0.008$, DMSO vs Jsp 0.5μm $p=0.004$; DMSO vs BS 50μm $p=0.003$.

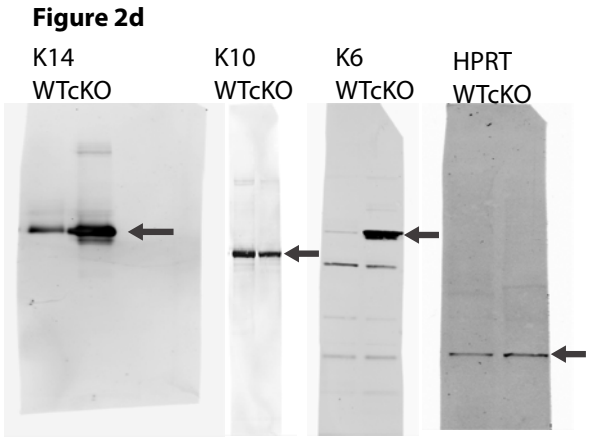

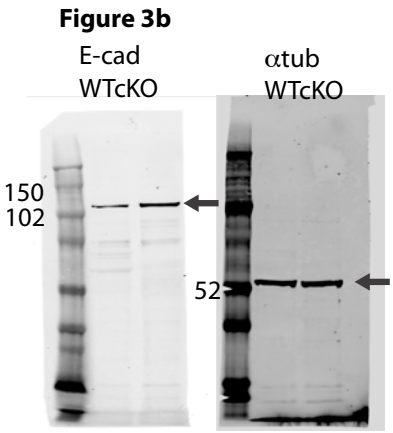

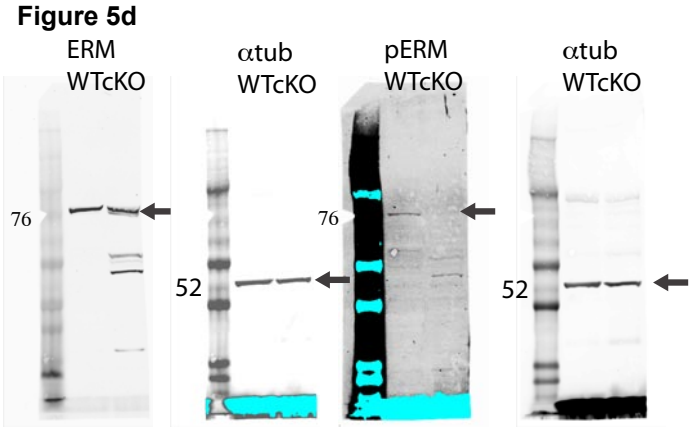

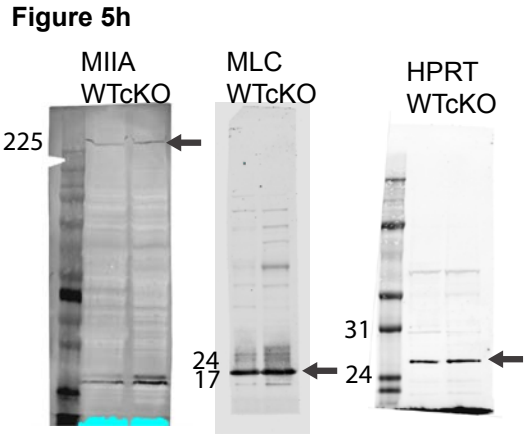

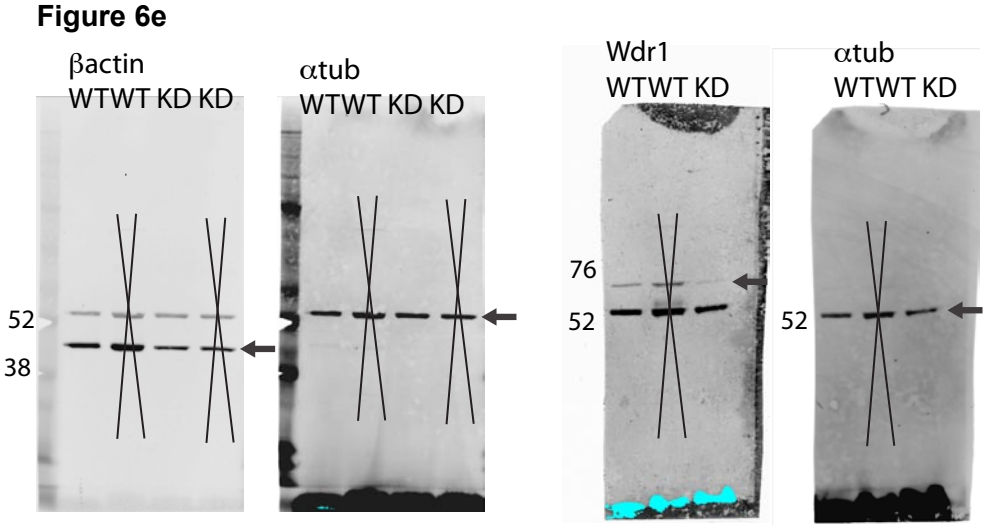

Figure S9 Full scans

Table S1. Summary of Microarray Analysis of decrease in Gene Expression in E16.5
***Srf* cKO vs WT Basal Cells.**
The listed probe sets were down regulated (fold change >1.5 and p<0.05) in the two independent experiment.

Probe Set	Gene Symbol	Gene Title	Mean fold change
1427682_a_at	Egr2	early growth response 2	9.09
1427683_at	Egr2	early growth response 2	8.12
1442067_at	---	---	6.73
1417065_at	Egr1	early growth response 1	5.05
1436329_at	Egr3	early growth response 3	3.88
1449141_at	Fblim1	filamin binding LIM protein 1	3.69
1425336_x_at	H2-K1	histocompatibility 2, K1, K region	3.22
1439183_at	Acer1	alkaline ceramidase 1	3.155
1450645_at	Mt4	metallothionein 4	3.14
1450981_at	Cnn2	calponin 2	3.14
1436448_a_at	Ptgs1	prostaglandin-endoperoxide synthase 1	2.96
1449204_at	Gjb5	gap junction protein, beta 5	2.62
AFFX-b-ActinMur/M12481_5_at	Actb	actin, beta	2.41
1457025_at	Sdr16c6	short chain dehydrogenase/reductase family 16C, member 6	2.39
1451263_a_at	Fabp4	fatty acid binding protein 4, adipocyte	2.38
1416930_at	Ly6d	lymphocyte antigen 6 complex, locus D	2.38
AFFX-b-ActinMur/M12481_M_at	Actb	actin, beta	2.32
1453568_at	Dapl1	death associated protein-like 1	2.30
1460330_at	Anxa3	annexin A3	2.30
1422587_at	Tmem45a	transmembrane protein 45a	2.22
1424701_at	Pcdh20	protocadherin 20	2.16
1437578_at	Clca2	chloride channel calcium activated 2	2.15
1417942_at	Lypd3	Ly6/Plaur domain containing 3	2.10
1451308_at	Elovl4	elongation of very long chain fatty acids (FEN1/Elo2, SUR4/Elo3, yea	2.08
1417928_at	Pdlim4	PDZ and LIM domain 4	2.08
1452679_at	Tubb2b	tubulin, beta 2B	1.99
1425810_a_at	Csrp1	cysteine and glycine-rich protein 1	1.94
1429808_at	1110020C03Rik ///	RIKEN cDNA 1110020C03 gene /// similar to CG4329-PA, isoform A	1.94
AFFX-b-ActinMur/M12481_3_at	Actb	actin, beta	1.94
1425811_a_at	Csrp1	cysteine and glycine-rich	1.93

1425811_a_at	Csrp1	cysteine and glycine-rich protein 1	1.93
1417408_at	F3	coagulation factor III	1.90
1456539_at	---	---	1.90
1427038_at	Penk	preproenkephalin	1.90
1436722_a_at	Actb	actin, beta	1.88
1424306_at	Elovl4	elongation of very long chain fatty acids (FEN1/Elo2, SUR4/Elo3, yea	1.86
1431211_s_at	Them5	thioesterase superfamily member 5	1.83
1424265_at	Npl	N-acetylneuraminate pyruvate lyase	1.83
1427910_at	Cst6	cystatin E/M	1.81
1424842_a_at	Arhgap24	Rho GTPase activating protein 24	1.81
1455519_at	Dsg1b	desmoglein 1 beta	1.80
1426677_at	Flna	filamin, alpha	1.75
1415779_s_at	Actg1	actin, gamma, cytoplasmic 1	1.74
1448312_at	Pcsk2	proprotein convertase subtilisin/kexin type 2	1.69
1423062_at	Igfbp3	insulin-like growth factor binding protein 3	1.69
1437591_a_at	Wdr1	WD repeat domain 1	1.68
1419734_at	Actb	actin, beta	1.68
1444254_at	Tns4	tensin 4	1.63
1431429_a_at	Arl4a	ADP-ribosylation factor-like 4A	1.63
1459898_at	Sbsn	suprabasin	1.63
1423054_at	Wdr1	WD repeat domain 1	1.63
1450851_at	Wdr1	WD repeat domain 1	1.62
1448318_at	Plin2	perilipin 2	1.57
1429297_at	Serpinb12	serine (or cysteine) peptidase inhibitor, clade B (ovalbumin), member	1.57
1427256_at	Vcan	versican	1.57
1437019_at	2200001I15Rik	RIKEN cDNA 2200001I15 gene	1.52
1419602_at	Hoxa2	homeo box A2	1.52

Table S2. Summary of Microarray Analysis of Increase in Gene Expression in E16.5
***Srf* cKO vs WT Basal Cells.**
The listed probe sets were up regulated (fold change >1.5 and p<0.05) in the two independent experiment.

1420491_at	Eif2s1	eukaryotic translation initiation factor 2, subunit 1 alpha	3.64
1418930_at	Cxcl10	chemokine (C-X-C motif) ligand 10	3.29
1442886_at	---	---	3.23
1442700_at	Pde4b	phosphodiesterase 4B, cAMP specific	2.33
1439780_at	Rpl7l1	ribosomal protein L7-like 1	2.23
1427932_s_at	1200003I10Rik /// 1200015M12Rik /// 1200016E24Rik /// A130040M12Rik /// E430024C06Rik	RIKEN cDNA 1200003I10 gene /// RIKEN cDNA 1200015M12 gene /// RIKEN cDNA 1200016E24 gene /// RIKEN cDNA A130040M12 gene /// RIKEN cDNA E430024C06 gene	2.14
1453238_s_at	1200016E24Rik /// 3930401B19Rik /// A130040M12Rik /// E430024C06Rik	RIKEN cDNA 1200016E24 gene /// RIKEN cDNA 3930401B19 gene /// RIKEN cDNA A130040M12 gene /// RIKEN cDNA E430024C06 gene	1.94
1448987_at	Acadl	acyl-Coenzyme A dehydrogenase, long-chain	1.83
1418230_a_at	Lims1	LIM and senescent cell antigen-like domains 1	1.81
1419721_at	Niacr1	niacin receptor 1	1.80
1417821_at	D17H6S56E-5	DNA segment, Chr 17, human D6S56E 5	1.80
1440681_at	Chrna7	cholinergic receptor, nicotinic, alpha polypeptide 7	1.75
1439200_x_at	---	---	1.70
1426951_at	Crim1	cysteine rich transmembrane BMP regulator 1 (chordin like)	1.69
1450971_at	Gadd45b	growth arrest and DNA-damage-inducible 45 beta	1.69
1416104_at	Mpdu1	mannose-P-dolichol utilization defect 1	1.68
1436983_at	Crebbp	CREB binding protein	1.62
1460713_at	BC048355	cDNA sequence BC048355	1.62
1452406_x_at	Erdr1	erythroid differentiation regulator 1	1.62
1416124_at	Ccnd2	cyclin D2	1.57
1450780_s_at	Hmga2	high mobility group AT-hook 2	1.57
1422851_at	Hmga2	high mobility group AT-hook 2	1.52
1429660_s_at	Smc2	structural maintenance of chromosomes 2	1.52
1418283_at	Cldn4	claudin 4	1.52
1455956_x_at	Ccnd2	cyclin D2	1.52

Table S3. Semi-Quantitative RT-PCR Primers table.

Gene	Forward primer	Reverse primer
HPRT	gatcagtcaacgggggacataaa	cttgcgctcatcttaggctttgt
Ppib	gtgagcgcttcccagatgaga	tgccggagtcgacaatgatg
Srf	gttgcccgccaccatcat	cgggcggatcattcactctt
itga6	ctggacacccgcgaggacaac	tcaaccggccatcgcagaaact
Krt14	cgccgcccctggtgtgg	atctggcggttggtggaggtca
Krt5	gttgaacgccgctgacct	cttcggaaggacacactggac
Notch1	caaactggcctgggtggggacat	aaaaggccagaaagagctgccctgag
Jag1	aagggaacagactgagctatatgactta	atttattgccaggaacaacacatcaaag
Pard6b	gggacctgccgcctataaataat	acacgggccggaagtcct
Pard6g	caagcctgggaagtttgaagattt	tgcggcatgctgatgttga
Prkcc	cagcgacagagaaaacttcctgaa	tcccgccatcatctcaaacata
Numa1	gtcaggccccttggagact	agcgggccagagactgagtg
Gpsm2	tctgctgcaaagagatccaaaca	tcatgggcaggtacaaaaagtcc
Myh9	cctgccataagggaacctaatcac	gcgctctggtgcctctccta
Fos	agagcgccccatccttacg	ggtgggctgccaaaataaactc
junb	acacaggcgcatctctgaagc	cggctccggaccagcata
Egr2	ggccgtagacaaaatcccagtaac	gaatttgcccatgtaagtgaaggtc
Egr1	atgtgggtggtaaggtggtcacta	aaccggcccagcaagaca
Nab2	gatccggaagtacagcgtcatcta	acttgtcgggacagtgagaagagtt
Gadd45a	tgccgggaaagtcgctacat	tttctcgcagcttccttcttcag
Gadd45b	tacgaggcggccaaactgat	tgatacccggacgatgtcaatg
Cnn2	aatgggcttcctgtttcttcatct	tcgtgggaaagcaaacttagtcc
Actb	cggccaggtcatcactattgg	aggggccggactcatcgta
Actg1	cccaaagctaacagagagaagatgacg	gtggtaaagctgtagccccgttca
Flna	gattggggaggagacggtgat	tttgctggctaccctgaggatag
Wdr1	tggagcggggcgtctcta	aatccgctgggtgcatacttg